

# Interfacial Slip in Sheared Polymer Blends

Tak Shing Lo<sup>1</sup>, Maja Mihajlovic<sup>2</sup>, \*Yitzhak Shnidman<sup>3,5</sup>, Wentao Li<sup>4</sup> and Dilip Gersappe<sup>4,5</sup>

<sup>1</sup>*The Levich Institute, City College of CUNY, New York, NY 10031*

<sup>2</sup>*Department of Chemistry, City College of CUNY, New York, NY 10031*

<sup>3</sup>*Department of Engineering Science and Physics,*

*College of Staten Island of CUNY, Staten Island, NY 10314*

<sup>4</sup>*Department of Materials Science and Engineering, SUNY, Stony Brook, NY 11794*

<sup>5</sup>*NSF MRSEC on Polymers at Engineered Interfaces*

(Dated: August 20, 2018)

We have developed a dynamic self-consistent field theory, without any adjustable parameters, for unentangled polymer blends under shear. Our model accounts for the interaction between polymers, and enables one to compute the evolution of the local rheology, microstructure and the conformations of the polymer chains under shear self-consistently. We use this model to study the interfacial dynamics in sheared polymer blends and make a quantitative comparison between this model and Molecular Dynamics simulations. We find good agreement between the two methods.

PACS numbers: 83.80.Tc, 83.50.Lh, 83.10.Rs

Self-consistent field (SCF) theory has been very useful for modeling and understanding the equilibrium properties of inhomogeneous polymer fluids. In lattice SCF theories, Markovian statistics for chains represented by lattice random walks are coupled with a mean field approximation for the free energy to determine variation of equilibrium properties across interfaces [1]. In contrast, interfacial dynamics and rheology of inhomogeneous polymer fluids driven out of equilibrium by applied stresses is still not well understood. Since experimental evidence indicates that the interfacial properties are critical to the evolution of the morphology of polymer blends, understanding the interplay between the interfacial dynamics and the polymer conformation at the interface is of great fundamental importance, and efficient computational models of these systems are essential for many industrial and biological applications.

We have recently developed a novel dynamic self-consistent field (DSCF) theory [2] by combining the lattice random walk formalism of Scheutjens and Fleer's static SCF model [1] and a convective-diffusive lattice gas model for simple compressible fluids [3]. As in static SCF theory, the distribution of free segments interacting with a self-consistent field representing adjacent connected segments and walls is approximated by a product of free segment (one-body) probabilities. The effect of flow on ideal chain conformations is modeled with FENE-P dumbbells, and related to stepping probabilities in a random walk. Free segment and stepping probabilities generate statistical weights for chain conformations in a self-consistent field, and determine local volume fractions of connected segments. Flux balance across a unit lattice cell yields mean-field transport equations for free segment probabilities and momentum densities. Diffusive and viscous contributions to the fluxes arise from segmental hops

modeled as a Markov process. Hopping transition rates depend on the changes in the free energy, reflecting segmental interactions, kinetic energy, and entropic contributions accounting for chain deformation under flow. It is the first dynamic mean-field theory for inhomogeneous polymer fluids that couples self-consistently the effects of flow, segmental and wall interactions, and compressibility on chain conformations, composition, transport and rheology in interfacial regions at the Kuhn length scale, which is necessary to resolve interfacial properties of typical polymer interfaces. This makes it different from other recently proposed approaches [4]. In this Letter, we focus on the interfacial dynamics of a symmetric polymer blend in the unentangled regime. We use the DSCF model to predict the velocity slip, chain conformations, and the reduction of shear viscosity across the interface between the coexisting polymer phases, and compare our results with molecular dynamics (MD) simulations.

We consider a blend of two immiscible homopolymer species A and B consisting of linear chains of  $N^A$  and  $N^B$  segments, respectively. The fluid is confined between two parallel walls normal to the  $z$ -axis in a Cartesian coordinate system at temperature  $T$ . The interface between the two polymers is parallel to, and is centered midway between the two walls. The walls move at equal and opposite velocities along the  $x$ -axis. We discretize the space between the two walls into triangular lattice layers parallel to the walls, stacked in a FCC lattice arrangement. The fluid system considered here is invariant under lattice translations in the  $xy$ -plane, and we simplify the DSCF equations utilizing this symmetry (see [2] for details).

Let  $P_i^\alpha$ ,  $\phi_i^\alpha$  and  $\mathbf{g}_i^\alpha$  be the free segment probability, segmental volume fraction and segmental momentum density of species  $\alpha$  ( $\alpha=A$  or  $B$ ) in each layer  $i$  ( $i=1, 2, \dots, L$ ), respectively. The free segment probabilities and the segmental momentum density  $\mathbf{g}_i = \mathbf{g}_i^A + \mathbf{g}_i^B$  evolve according to

$$\frac{dP_i^\alpha}{dt} = -\nabla \cdot (P_i^\alpha \mathbf{u}_i) - \left( \frac{\mathbf{j}_i^\alpha - \mathbf{j}_{i-1}^\alpha}{\sqrt{2/3}a} \right) \cdot \hat{\mathbf{z}} \quad (1)$$

\*Corresponding author. E-mail: shnidman@mail.csi.cuny.edu

and

$$\frac{d\mathbf{g}_i}{dt} = \sum_{\alpha=A,B} [-\nabla \cdot (\mathbf{g}_i^\alpha \mathbf{u}_i + \varepsilon_i^\alpha) - \left( \frac{\pi_i^\alpha - \pi_{i-1}^\alpha}{\sqrt{2/3}a} \right) \cdot \hat{\mathbf{z}} - \frac{\phi_i^\alpha}{wP_i^\alpha} (\zeta_{i,i+1}^\alpha \mathbf{j}_i^\alpha + \zeta_{i,i-1}^\alpha \mathbf{j}_{i-1}^\alpha)], \quad (2)$$

which are obtained by applying mass and momentum conservation laws to a rectangular control volume of  $w=a^3/\sqrt{2}$  centered at a site in layer  $i$ . Here  $\zeta_{i,i\pm 1}^\alpha$  is the locally averaged segmental friction coefficient of species

$\alpha$  (see [2] for details) and  $\mathbf{u}_i = \mathbf{g}_i w / (m^A \phi_i^A + m^B \phi_i^B)$ , where  $m^\alpha$  is the segmental mass of species  $\alpha$ , is the mass averaged velocity at a site in layer  $i$ . The tensor  $-\varepsilon_i^\alpha$  in Eq. (2) represents the elastic contribution to the stress and is defined in [2]. Let  $D_{i,i+1}^\alpha = k_B T / N^\alpha \zeta_{i,i+1}^\alpha$  and  $\nu_{i,i+1}^\alpha = \zeta_{i,i+1}^\alpha a^2 / 24m^\alpha$  be the locally averaged self-diffusion coefficient and kinematic viscosity of species  $\alpha$ , and  $\bar{\phi}$  be the overall average polymer volume fraction, the diffusive free segment probability current and the viscous stress tensor at the mid-plane between layers  $i$  and  $i+1$  in Eqs. (1) and (2) are given by

$$\mathbf{j}_i^\alpha = 3\sqrt{\frac{2}{3}} \frac{(1 - \delta_{i+1,1})(1 - \delta_{i,L})}{(1 - \bar{\phi})} \frac{D_{i,i+1}^\alpha}{a} \left[ P_i^\alpha (1 - \phi_{i+1}) \varphi \left( \frac{\Delta \langle H_i^\alpha \rangle}{k_B T} \right) - P_{i+1}^\alpha (1 - \phi_i) \varphi \left( \frac{-\Delta \langle H_i^\alpha \rangle}{k_B T} \right) \right] \hat{\mathbf{z}} \quad (3)$$

and

$$\pi_i^\alpha = 3\sqrt{\frac{2}{3}} \frac{(1 - \delta_{i+1,1})(1 - \delta_{i,L})}{(1 - \bar{\phi})} \frac{m^\alpha \nu_{i,i+1}^\alpha}{w a} \left[ \phi_i^\alpha \mathbf{u}_i (1 - \phi_{i+1}) \varphi \left( \frac{\Delta \langle H_i^\alpha \rangle}{k_B T} \right) - \phi_{i+1}^\alpha \mathbf{u}_{i+1} (1 - \phi_i) \varphi \left( \frac{-\Delta \langle H_i^\alpha \rangle}{k_B T} \right) \right] \hat{\mathbf{z}}. \quad (4)$$

In Eqs. (3) and (4),  $\varphi$  is the Kawasaki transition rate function  $\varphi(x) = 2/(1 + e^x)$  [5] which satisfies local detailed balance, and  $\Delta \langle H_i^\alpha \rangle = \langle H_{i+1}^\alpha \rangle - \langle H_i^\alpha \rangle$  is the free energy change due to a hop of a segment of species  $\alpha$  from layer  $i$  to  $i+1$ . The local contribution to the free energy of a segment of species  $\alpha$  in layer  $i$  is

$$\begin{aligned} \langle H_i^\alpha \rangle &= \sum_{\beta=A,B} \frac{(1 - \delta_{\alpha\beta})}{2} \chi_{AB} \langle \langle \phi_i^\beta \rangle \rangle - \chi_s^\alpha (\delta_{i1} + \delta_{iL}) \\ &+ \frac{m^\alpha}{2} \phi_i^\alpha \mathbf{u}_i^2 - \frac{\phi_i^\alpha k_B T}{2N^\alpha} \left[ \text{Tr} \left( \mathbf{I} - \frac{3}{N^\alpha a^2} \mathbf{S}_i^\alpha \right) \right. \\ &\left. + \ln \det \left( \frac{3}{N^\alpha a^2} \mathbf{S}_i^\alpha \right) \right] \end{aligned} \quad (5)$$

where  $\chi_{AB}$  is the segment-segment interaction parameter for species  $A$  and  $B$ , and  $\chi_s^\alpha$  is the segment-wall interaction parameter of a segment of species  $\alpha$ . In Eq. (5), the double angular brackets represent summation over all nearest neighbors of a site in layer  $i$  and  $\mathbf{S}_i^\alpha$  is the second moment of the end-to-end vector of an ideal (non-interacting)  $\alpha$ -type chain under flow, with its center-of-mass being in the  $i$ th layer. The last two terms in Eq. (5) are contributions from the kinetic energy and the free energy change due to stretching of the chains.

The conformations of interacting polymer chains are generated by lattice random walks in a self-consistent field modeling these interactions. According to [1], the segmental volume fraction are obtained from the free segment probability by

$$\phi_i^\alpha = \frac{\bar{\phi}^\alpha L}{N^\alpha \sum_{j=1}^L P_j^\alpha(N^\alpha)} \sum_{s=1}^{N^\alpha} \frac{P_i^\alpha(s) P_i^\alpha(N^\alpha - s + 1)}{P_i^\alpha / (1 - P_i^A - P_i^B)} \quad (6)$$

where

$$\begin{aligned} P_i^\alpha(s) &= P_i^\alpha [\lambda_{+,i-1}^\alpha P_{i-1}^\alpha(s-1) + \lambda_{0,i}^\alpha P_i^\alpha(s-1) \\ &+ \lambda_{-,i+1}^\alpha P_{i+1}^\alpha(s-1)] / (1 - P_i^A - P_i^B) \end{aligned} \quad (7)$$

for  $s = 2, 3, \dots, N^\alpha$  and  $P_i^\alpha(1) = P_i^\alpha / (1 - P_i^A - P_i^B)$ . In Eq. (6),  $\bar{\phi}^\alpha$  is the average volume fraction of species  $\alpha$  in the system and in Eq. (7),  $\lambda_{\pm,i}^\alpha$  is the stepping probability of a  $\alpha$ -type segments in an ideal chain from layer  $i$  to layer  $i \pm 1$ , whereas  $\lambda_{0,i}^\alpha$  is the stepping probability from a site in layer  $i$  to a nearest neighbor in the same layer. In contrast to the static SCF theory, these probabilities are now time-dependent and anisotropic, and are related to the components of  $\mathbf{S}_i^\alpha$  through the random walk picture (see [2]).

Finally,  $\mathbf{S}_i^\alpha$  evolves according to

$$\begin{aligned} \frac{D\mathbf{S}_i^\alpha}{Dt} &- (\nabla \mathbf{u}_i)^\text{T} \cdot \mathbf{S}_i^\alpha - \mathbf{S}_i^\alpha \cdot (\nabla \mathbf{u}_i) \\ &= -\frac{1}{\tau_{db,i}^\alpha} \left[ \frac{\mathbf{S}_i^\alpha}{1 - \frac{1}{N^\alpha(N^\alpha-1)a^2} \text{Tr} \mathbf{S}_i^\alpha} - \frac{N^\alpha a^2}{3} \mathbf{I} \right], \end{aligned} \quad (8)$$

which is the constitutive equation of the FENE-P dumbbell model [6], but with the value of the spring constant chosen in such a way that  $\mathbf{S}_i^\alpha$  reverts to the Hookean dumbbell value in equilibrium. In Eq. (8),  $\tau_{db,i}^\alpha = N^\alpha \zeta_i^\alpha a^2 / 24k_B T$  is the local dumbbell relaxation time where  $\zeta_i^\alpha$  is the local segmental friction coefficient of species  $\alpha$ , which is related to the one in the bulk through the Doolittles' law [7] (see [2] for details).

In the actual computation, all spatial derivatives are approximated by using finite difference formulas. Under suitable boundary conditions, Eqs. (1), (2) and (8) form a closed system of ordinary differential equations, which is solved numerically.

Henceforth we focus on symmetric blends, i.e.  $N^A = N^B = N$ ,  $m^A = m^B = m$ , and the two polymers A and B have the same density and segmental friction coefficient. We also set  $\chi_s^A = \chi_s^B = 0$ . We shall compare the numerical solutions of the DSCF equations with Molecular Dynamics (MD) simulations of a similar system. The details of the model and the method of the MD simulation that we used can be found in [8]. In MD, the characteristic energy ( $\epsilon$ ), time ( $\tau$ ) and length ( $\sigma$ ), and the segmental mass ( $m$ ) are related by  $\tau = \sigma\sqrt{m/\epsilon}$ . As in [8], we set the temperature in our MD simulations by  $\epsilon = k_B T/1.1$ .

In order to compare our model to MD simulations, we have to establish the relationships between the model parameters in the DSCF theory and those in MD. The Kuhn length in the MD simulations is estimated to be  $a \approx 1.3\sigma$  [8], hence, one Kuhn segment is equivalent to 1.3 beads in MD. The interaction parameter  $\chi_{AB}$  is obtained by fitting the equilibrium density profiles calculated from DSCF theory to the ones obtained from MD. After accounting for capillary wave broadening of the intrinsic profiles in MD simulations [9], this gives  $12\chi_{AB}/k_B T \approx 1.1$ . The segmental friction coefficient in the bulk is obtained by comparing the self-diffusion constants calculated from MD to the one in our model. The segmental mass in our model is identical to the one used in MD. In the simulations, we set  $\bar{\phi}^A = \bar{\phi}^B$  and the overall polymer volume fraction averaged over the simulation box to  $\bar{\phi} = \bar{\phi}^A + \bar{\phi}^B = 0.85$ . This average volume fraction is used both in the DSCF model and MD simulations.

As the first test of the DSCF model, we calculated the steady state velocity profiles and the local viscosities between the walls under shear for different chain lengths, and compared them with the MD results. The steady state is obtained by integrating the DSCF equations of motion in time under a constant rate for shearing the two walls (nominal shear rate), starting from equilibrium.

The shear velocity profile (defined as the local mass-averaged velocity) across the polymer-polymer interface in the middle of the channel from our model for  $N=12$  is shown in the left panel of Fig. 1. The result from MD simulations using chains of 16 beads is also shown. The shear rates  $\dot{\gamma}$  in the bulk are indicated in the caption [10]. This bulk shear rate is obtained by fitting the linear part of the velocity profile to a straight line and is different from the nominal shear rate because of the velocity slip at the walls and the interface. Note that a kink representing a velocity slip at the interface is observed here. This interfacial slip phenomenon was first predicted by de Gennes [11] based on a scaling argument, and later modeled with an approximate constitutive equation for incompressible polymer blends by Goveas and Fredrickson [12], and was subsequently confirmed by Barsky and Robbins [13] using MD. Experimental studies have also indicated the presence of a velocity slip at the interface in polymer blends [14]. Here the same velocity slip is produced in our DSCF model. The bulk shear rates for the DSCF and MD results shown in Fig. 1 are not identical, but the closest that we can attain. This is because

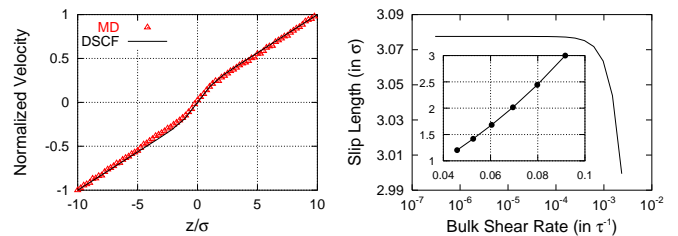


FIG. 1: Left: Steady state shear velocity profile for  $N=12$  obtained from DSCF at  $\dot{\gamma}=2.36 \times 10^{-3} \tau^{-1}$  and MD at  $\dot{\gamma}=4.04 \times 10^{-3} \tau^{-1}$ . (The velocity is normalized by the velocity at  $z = 10\sigma$ .) Right: Variation of slip length with shear rate and with  $\chi_{AB}$  for  $N=12$  obtained from DSCF. (Inset shows the slip length in  $\sigma$  Vs  $\chi_{AB}/k_B T$  at nominal shear rate  $2.75 \times 10^{-3} \tau^{-1}$ .)

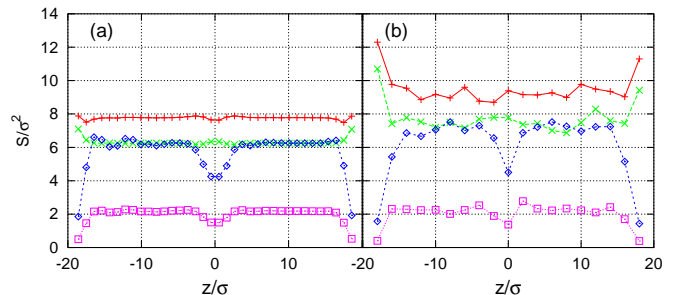


FIG. 2: Second moment of the end-to-end distance for  $N=12$  obtained from (a) DSCF at  $\dot{\gamma}=2.36 \times 10^{-3} \tau^{-1}$ , and (b) MD at  $\dot{\gamma}=4.04 \times 10^{-3} \tau^{-1}$ . (+:  $S_{xx}$ ,  $\times$ :  $S_{yy}$ ,  $\diamond$ :  $S_{zz}$ ,  $\square$ :  $S_{xz}$ .)

simulating systems with low shear rates in MD is not computationally feasible. On the other hand, the DSCF simulations currently become unstable at higher shear rates, though they cover most experimentally accessible shear rates.

To quantify the interfacial slip, we calculated the slip length, which is defined as twice the magnitude of the  $x$ -intercept of the straight line obtained from a linear fit to the linear part of the steady state velocity profile. The results are shown in the right panel of Fig. 1. Our model shows that the slip length decreases as the shear rate increases. We verified this result by performing MD simulations of the same system at two different bulk shear rates: one at  $4.04 \times 10^{-3} \tau^{-1}$  and the other one at  $8.27 \times 10^{-3} \tau^{-1}$ . The slip lengths were found to be  $1.95\sigma$  and  $1.22\sigma$ , respectively. The trend is the same as the one predicted by the DSCF model. We also calculated the slip length as a function of  $\chi_{AB}$  at a fixed nominal shear rate and the result is shown in the inset of the same figure. It shows that the slip length increases as the strength of the segment-segment interaction increases. A similar qualitative trend was also observed by using MD in earlier studies [13].

We also calculated the second moment of the end-to-end vector at steady state by performing a Monte-Carlo simulation of lattice random walks in a self-consistent field representing conformations of interacting chains under shear. The transition rates used in the Monte-Carlo simulation were constructed from the stepping and free

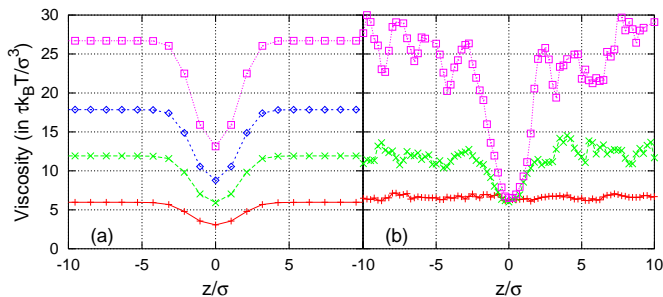


FIG. 3: Steady state viscosity profiles across the polymer-polymer interface for different chain lengths obtained from (a) DSCF at nominal shear rate  $6.24 \times 10^{-4} \tau^{-1}$ , and (b) MD at various nominal shear rates. (+:  $N=6$ ,  $\times$ :  $N=12$ ,  $\diamond$ :  $N=18$ ,  $\square$ :  $N=24$ .)

segment probabilities from the DSCF theory. The result is shown in Fig. 2 and compared to the one obtained from MD. In the bulk, we have good agreement between the two simulations. The slight difference can be accounted for by the difference in the shear rates. In the interfacial region, our model predicts the same trend as in MD. Similar results were also obtained by Barsky and Robbins in [15] using MD.

The steady state viscosity profiles in the interfacial region for various chain lengths are calculated by dividing the viscous shear stress by the local shear rate, and are shown in Fig. 3(a). Note that a drop in the viscosity occurs at the polymer-polymer interface and it is more pronounced for longer chains. Corresponding results from MD are shown in Fig. 3(b). Here one can see that the trend predicted by the DSCF model is in general agreement with the MD results. The shear viscosities obtained from both methods in the bulk regions are very close. In

the interfacial region, the drop is underestimated for long chains and slightly overestimated for short chains in the DSCF model, but the general agreement is very good given all the approximations of the model. A similar drop in the viscosity was also observed by Barsky and Robbins using MD [13], but with different parameters.

We have studied the interfacial slip phenomenon in phase separated sheared polymer blends using the novel DSCF theory and compared our results with MD simulations. Good agreement between the two approaches is found. For unentangled polymer fluids studied here, the DSCF simulation time is only a small fraction of that in MD. We expect that these computational efficiencies will be more manifest in the case of entangled polymer fluids, for which MD simulations are currently impractical. The current DSCF theory is based on conservation laws for species occupancies and momentum that are coupled to models of polymer structure and conformation. It can be generalized either by changing the constitutive stress equation (accounting for the reptation regime), the polymer model (e.g., accounting for block copolymers or branching) or by incorporating additional conservation laws (e.g., for energy and/or charge). Work along these lines will be reported in future publications.

This work was supported by the Mitsubishi Chemical Corporation of Japan. M. Mihajlovic and Y. Shnidman would also like to acknowledge support by a grant from the National Science Foundation (DMR-0080604). We would like to acknowledge useful discussions with Drs. G. Fredrickson and D. Wu. We thank Dr. T. Kawakatsu for sending his preprint prior to its publication. The work of the first three authors was performed at Polytechnic University in Brooklyn.

- 
- [1] J. Scheutjens and G.J. Fleer, *J. Phys. Chem.* **83**, 1619 (1979).
- [2] M. Mihajlovic, T.S. Lo and Y. Shnidman. (submitted to *Macromolecules*); M. Mihajlovic, Ph.D. thesis, Polytechnic University (2004).
- [3] A.A. Khan and Y. Shnidman, *Progr. Colloid. Polym. Sci.* **103**, 251 (1997).
- [4] N.M. Maurits, A.V. Zvelindovsky and J. Fraaije, *J. Chem. Phys.* **109**, 11032 (1998); G.H. Fredrickson, *J. Chem. Phys.* **117**, 6810 (2002); T. Shima, H. Kuni, Y. Okabe, M. Doi, H.F. Yuan and T. Kawakatsu, *Macromolecules* **36**, 9199 (2003).
- [5] B. Schmittmann and R.K.P. Zia, *Statistical Mechanics of Driven Diffusive Systems*. (Academic Press, London, 1995).
- [6] R. Bird, C. Curtiss, R. Armstrong and O. Hassager, *Dynamics of Polymeric Liquids, 2nd Ed, Vol. 2*. (John Wiley & Sons, 1987); M. Herrchan and H.C. Ottinger, *J. Non-Newtonian Fluid Mech.* **68**, 17 (1997).
- [7] A.K. Doolittle and D.B. Doolittle, *J. Appl. Phys.* **28**, 901 (1957).
- [8] K. Kremer and G. Grest, *J. Chem. Phys.* **92**, 5057 (1990).
- [9] A.N. Semenov, *Macromolecules* **27**, 2732 (1994); M.D. Lacasse, G.S. Grest and A.J. Levine, *Phys. Rev. Lett.* **80**, 309 (1998); K. Binder, M. Muller, F. Schmid and A. Werner, *Adv. Coll. Interf. Sci.* **94**, 237 (2001).
- [10] In comparing DSCF results with the MD simulations, we made sure that the MD simulations were operating in a range in which the shear stress is independent of shear rate. This allows us to compare the two methods, even though the shear rates are not identical.
- [11] P.G. de Gennes, *C.R. Acad. Sci.* **308 II**, 1401 (1989); F. Brochard, P.G. de Gennes and S. Troian, *C.R. Acad. Sci. Paris* **310 III**, 1169 (1990).
- [12] J.L. Goveas and G.H. Fredrickson, *Eur. Phys. J. B* **2**, 79 (1998).
- [13] S. Barsky and M.O. Robbins, *Phys. Rev. E*, **63**, 021801 (2001).
- [14] R. Zhao and C.W. Macosko, *J. Rheol.*, **46**(1), 145 (2002).
- [15] S. Barsky and M.O. Robbins, *Phys. Rev. E*, **65**, 021808 (2002).